International Journal of Thermophysics, Vol. 19, No. 1, 1998

Radiant Power Exchange in Thermal Radiation Calorimetry

K. Hisano,[1,2] S. Sawai,[1] and K. Morimoto[1]

Received July 21, 1997

Radiant power exchange for thermal radiation calorimetry was investigated both theoretically and experimentally. The geometrical relation in which a disk-shaped copper specimen and a graphite plate are facing each other was used as the model configuration. Surfaces of the specimen and the plate were blackened with colloidal graphite to achieve a high surface emissivity. The radiant power density absorbed by the specimen was calculated by taking into account the geometrical configuration factors and the total emissivity of the blackened surfaces obtained form spectral reflectivity. A value of 0.56 ± 0.01 was obtained for the radiant power exchange coefficient from the theoretical results in the temperature range from 220 to 430°C. The coefficient obtained experimentally by use of a heat capacity measurement was constant with temperature, with a value of 0.54 ± 0.01 within experimental error. No hysteresis in the coefficient was observed for either heating or cooling processes.

KEY WORDS: calorimetry; emissivity; heat capacity; high temperature; radiant exchange.

1. INTRODUCTION

Thermal radiation calorimetry has been developed for measurements of the specific heat capacity [1, 2] and thermal conductivity [3, 4] of a solid specimen. In this calorimetry, a disk-shaped specimen and a heater are mounted in a vacuum chamber, with the specimen heated by irradiation. The specimen surfaces are blackened to achieve the same high emissivity for all measured specimens. The radiant power exchanged between the specimen and the heater is proportional to the difference in the fourth

[1] Department of Mathematics and Physics, National Defense Academy, Hashirimizu 1-10-20, Yokosuka 239, Japan.

[2] To whom correspondence should be addressed.

0195-928X/00/0700-0305$18.00/0

power of the temperatures. The exchange coefficient is constant as long as the geometrical relation between the heater and the specimen and the emissivity are the same. So far, the coefficient has been confirmed to be constant only experimentally by use of a heat capacity measurement of a high-conductivity specimen whose specific heat capacity is known at various temperatures. It is also worthwhile to discuss the exchange coefficient theoretically to confirm the validity and reliability of the thermal radiation calorimetry.

In this paper, the exchange coefficient is calculated by taking account of the configuration between the heater and the specimen and of the spectral emissivity of the specimen surface. The results are also compared with those obtained experimentally using a copper specimen.

2. THERMAL RADIATION CALORIMETRY

Let us consider the situation in which a thin specimen is heated at one face by thermal radiation from a flat heater (Fig. 1a). For the heat capacity measurement, the following equation for the specimen is proposed [1, 2]:

$$MC_p \frac{dT_s}{dt} = E_h A(I_h - I_s) - E_s A(I_s - I_r) - \frac{dQ_s}{dt} \tag{1}$$

where M, A, and C_p are the mass, the surface area, and the specific heat capacity of the specimen, respectively. I is equal to σT^4, where σ is the Stefan–Boltzmann constant. dT_s/dt is the change rate of the specimen temperature. dQ_s/dt is the heat loss per unit time through the specimen suspensions. Subscripts s, h, and r refer to the specimen, the heater, and the chamber wall, respectively. E_h is the "effective" emissivity expressing the radiant power exchange coefficient, which is defined in the present paper. E_s is also the effective emissivity related to the coefficient for the radiant power leaving the specimen to the chamber wall from the specimen back surface facing the chamber wall and from the front surface facing the heater. From Eq. (1), the following relation is derived at the same specimen temperature by considering the processes for both heating and cooling as long as E_h is the same for both processes:

$$\frac{C_p}{E_h} = \frac{A_s(I_h - I'_h)}{M((dT_s/dt) - (dT'_s/dt))} \tag{2}$$

where superscript ′ indicates the cooling mode. dQ_s/dt is largely canceled because of the same temperature. Equation (2) shows that the specific heat capacity is obtained from the value of the effective emissivity because

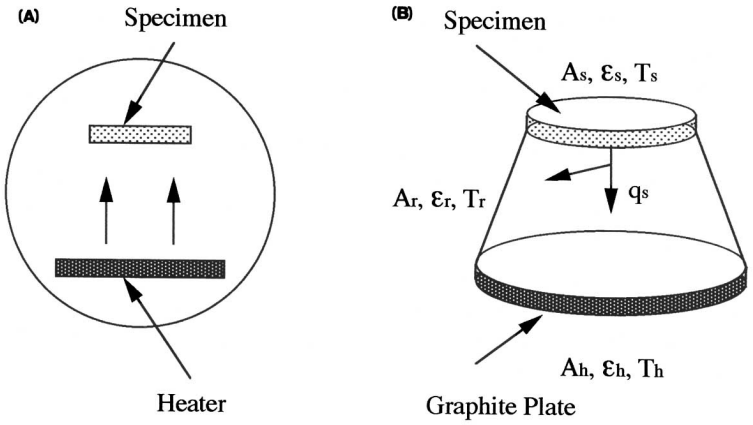

Fig. 1. (a) Schematic diagram of thermal radiation calorimetry. A flat heater and a disk-shaped specimen are mounted in a vacuum chamber. (b) Model geometrical configuration for calculation of the radiant power exchange coefficient A, ε, and T are the surface area, the emissivity, and the temperature, respectively. q_s is the radiant power density emitted from the specimen.

all quantities on the right-hand side of the equation are measurable. Conversely, the emissivity is obtained if we know the heat capacity. The technique of using a measurement for both processes was applied first for simultaneous measurement of the heat capacity and the total hemispherical emissivity of electrical conductive materials at high temperatures in Ref. 5, as far as the present authors are aware.

3. RADIANT POWER EXCHANGE

A method to calculate the radiant power exchange between hotter and cooler plates facing each other has already been established [6, 7]. The geometrical configuration for disk-shaped plates shown in Fig. 1b is used for the calculation. The side surface, which is necessary to make the system a closed surface, is assumed to be perfectly insulated and to have a perfectly absorbing surface ($\varepsilon_r = 1$). This model configuration matches the situation in the inside chamber of the thermal radiation calorimeter. If we assume also that the surfaces of both plates are rough and retain a high constant emissivity with temperature (gray surface), the reciprocity among the geometrical configuration factors is valid. That is,

$$A_s F_{s-h} = A_h F_{h-s} \tag{3}$$

where F_{s-h} is the configuration factor giving the fraction radiant power leaving gray surface s that arrives at gray surface h. The relations among the factors are given as

$$F_{h-s}+F_{h-r}=1 \tag{4}$$

$$F_{s-h}+F_{s-r}=1 \tag{5}$$

The calculation of the factor F_{h-s} for the present configuration is also described in the literature [7]. It is given by the solution of the following equation:

$$A_h F_{h-s}^2-(A_h+A_s+\pi d^2)\,F_{h-s}+A_s=0 \tag{6}$$

where d is the distance between the plates. The results of the calculation using the method described in the literature [6, 7] show that the radiant power per unit area (power density) q_s leaving surface s is given as

$$q_s=\frac{1}{D}\left[-F_{s-h}I_h+\frac{1}{\varepsilon_h}\{1-F_{h-s}F_{h-r}(1-\varepsilon_h)\}\,I_s -\frac{1}{\varepsilon_h}\{F_{s-h}F_{h-r}(1-\varepsilon_h)+F_{s-r}\}\,I_r\right] \tag{7}$$

where $D=(1/\varepsilon_h\varepsilon_s)-F_{h-s}F_{s-h}(1-(1/\varepsilon_h))(1-(1/\varepsilon_s))$. ε_h and ε_s are the total emissivities of the plates. We may rewrite the above equation as follows:

$$q_s=\frac{1}{D}\left[-F_{s-h}(I_h-I_s)+\frac{1}{\varepsilon_h}\{1-\varepsilon_h F_{s-h}-(1-\varepsilon_h)\,F_{s-h}F_{h-s}\}(I_s-I_r)\right] \tag{8}$$

The first term on the right-hand side of Eq. (8) indicates the radiant power density absorbed by surface s, while the second term is the density emitted to the side wall r. Therefore, the emissivities E_h and E_s in Eq. (1) are expressed as

$$E_h=\frac{F_{s-h}}{D} \tag{9}$$

$$E_s=\frac{1}{D}\left\{\frac{1}{\varepsilon_s}-F_{s-h}-\left(\frac{1}{\varepsilon_s}-1\right)F_{s-h}F_{h-s}\right\}+\varepsilon_s \tag{10}$$

The second term on the right-hand side of the above equation is the emissivity of the back specimen surface, which is assumed to be the same as that of the front surface.

4. EXPERIMENTAL

4.1. Apparatus

Figure 2 shows the schematic setup of the heater part used in the present experiment. This part is set in a water cooled vacuum chamber (20 cm in diameter and 25 cm long) with the inside blackened with colloidal graphite. A vacuum is maintained at better than 10^{-3} Pa. A graphite plate (27 mm in diameter and 0.6 mm thick) with an attached alumel–chromel thermocouple (0.1 mm in diameter) is heated using a graphite sheet heater (50 mm square and 0.3 mm thick) covered with copper radiation shields. The specimen and the graphite plate are blackened with colloidal graphite (Electrodag 188, Acheson) at a density of 2 mg $\cdot$ cm^{-2} to achieve the same emissivity. As a result of blackening, the surfaces become velvet-like after evaporating the acrylic binder above 400°C. The copper specimen (25 mm in diameter and 2 mm thick) is heated on one face by irradiation from the graphite plate. The heater current is controlled so that the temperature change rate of the copper specimen is approximately 5°C $\cdot$ min^{-1} for both heating and cooling modes. The gap distance d is maintained at 7 mm. Equations (3) and (6) give values of 0.541 and 0.631 for the present configuration factors of F_{h-s} and F_{s-h}, respectively.

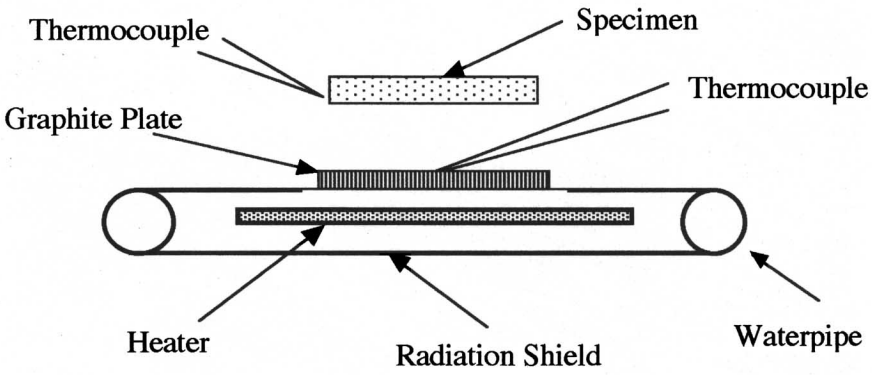

Fig. 2. Schematic diagram for the heater part. A graphite plate is heated by irradiation from the heater.

4.2. Emissivity

A room-temperature SEM photograph of the blackened surface taken by tilting the surface 80° from the normal direction is shown in Fig. 3. The surface shows a roughness of about 10 μm in both height and width. Figure 4 shows the specular and diffuse reflection spectra of the surface measured at room temperature using a Brucker 113v FTIR spectrometer. The specular reflection spectrum was measured at an incident angle of 15°. It was not possible to obtain the diffuse reflection spectrum in the far-infrared region because of weak infrared signals. The reflectivity is less than 10% below a 10-μm wavelength as shown in Fig. 4. Because of the rough and low-reflectivity surface, the temperature dependence of the total emissivity can be calculated assuming the spectral emissivity $\varepsilon(\lambda)$ to be equal to $1 - R_s(\lambda) - R_d(\lambda)$, where λ and $R(\lambda)$ are the wavelength and the reflectivity, respectively. That is,

$$\varepsilon(T) = \frac{\int_0^\infty \varepsilon(\lambda)\, w(\lambda, T)\, d\lambda}{\sigma T^4} \approx \frac{\int_1^{100\,\mu\mathrm{m}} \varepsilon(\lambda)\, w(\lambda, T)\, d\lambda}{\int_1^{100\,\mu\mathrm{m}} w(\lambda, T)\, d\lambda} \tag{11}$$

where $w(\lambda, T)$ is Planck's spectral distribution of emissive power. Figure 5 shows the temperature dependence of the total emissivity calculated from

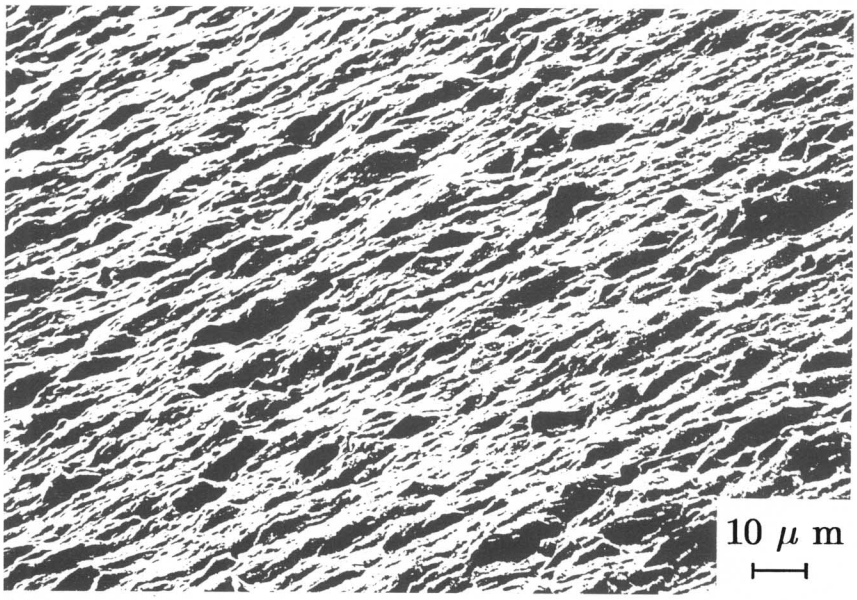

Fig. 3. SEM photograph of the specimen surface blackened with colloidal graphite.

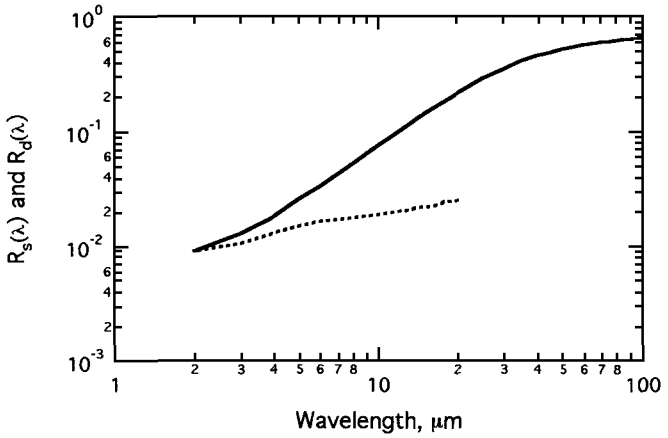

Fig. 4. Specular and diffuse reflection spectra of the specimen surface blackened with colloidal graphite. Solid line, specular reflection $R_s(\lambda)$. Dashed line, diffuse reflection $R_d(\lambda)$.

Eq. (11). The emissivity becomes higher than 90% and shows a small change above 220°C. In the calculation, the reflectivity between 1- and 2-μm wavelengths was assumed to maintain the value of 2 μm and the diffuse reflectivity beyond 20 μm was assumed constant at a value of 20 μm.

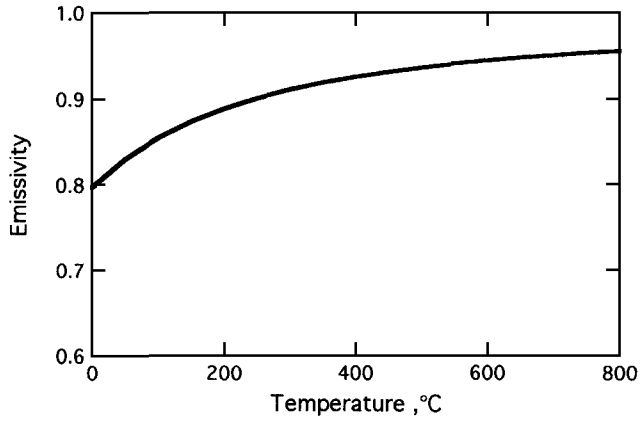

Fig. 5. Total emissivity of the blackened specimen surface calculated from Eq. (11).

5. RESULTS AND DISCUSSION

Collection of the data set for T_s and T_h was performed for heating and cooling modes with data collected every 15 s, with an interval of about 1.25°C between the data points. Figure 6 shows the graphite-plate temperature and the temperature difference between the modes at various specimen temperatures. This difference changes from 35 to 13°C in this temperature range. The temperature change rate is plotted for both modes in Fig. 7. The experimental "effective" emissivity estimated from Eq. (2) using data for the specific heat capacity of copper taken from the literature [8] is shown in Fig. 8. It is seen that E_h is almost constant with temperature, with a value of 0.54 ± 0.01. Hysteresis of E_h in both modes was not observed within experimental error, which was confirmed by the measurement of the plate temperature at equilibrium. Table I lists E_{h0} and E'_{h0} at several specimen temperatures obtained from the results at equilibrium and transient states by giving one of the terms of the change rate in Eq. (2) the value of zero. T_{h0} is the plate temperature at equilibrium. It is now possible to obtain the theoretical effective emissivity from Eq. (9) since T_s, $T_h(T_s)$, $\varepsilon(T_h)$, and $\varepsilon(T_s)$ are given by the results shown in Figs. 5 and 6. Strictly speaking, since the spectral emissivity is not constant with wavelength, the spectral radiant power density $q_s(\lambda)$ in Eq. (8) has to be considered. However, because the present rough surfaces maintain a high total emissivity with a small temperature change above 200°C, it is a good approximation to derive the value from Eq. (9).

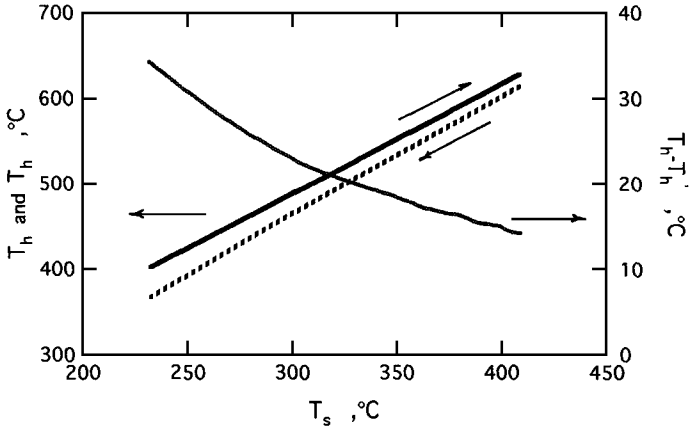

Fig. 6. Graphite-plate temperatures for heating and cooling modes and the temperature difference between the modes at various temperatures.

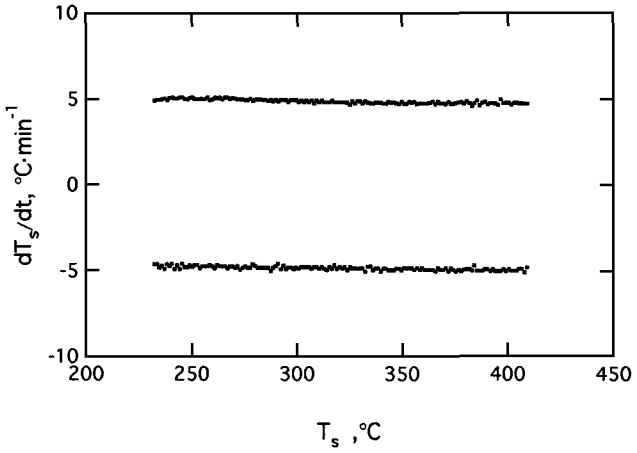

Fig. 7. Rate of temperature change for heating and cooling modes at various temperatures.

Figure 8 also includes the results calculated at various temperatures. The theoretical effective emissivity is fairly constant with temperature with a value of 0.56 ± 0.01. This small difference between the theory and the experiment is not clearly understood. However, the configuration factor is quite sensitive to the distance d between the plates and the emissivity is based on the room temperature reflectivity of the blackened surface. The

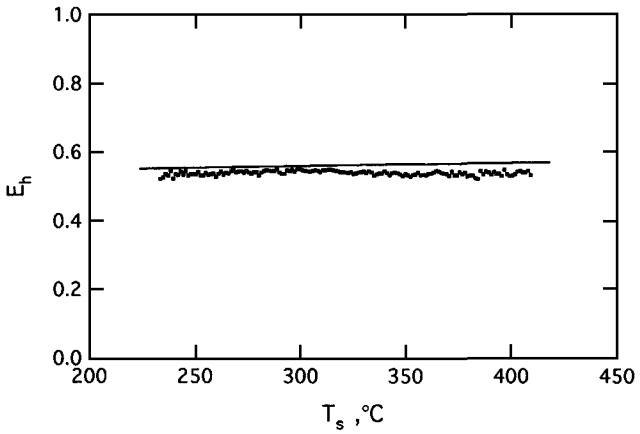

Fig. 8. Temperature dependence of the radiant power exchange coefficient (the "effective" emissivity) obtained experimentally from Eq. (2). The solid line indicates the coefficient obtained theoretically from Eq. (9).

Table I. Experimental and Calculated Radiant Power Exchange Coefficients and Specimen and Graphite-Plate Temperatures[a]

T_s	T_h	T_{h0}	T'_h	E_{h0}(exp)	E'_{h0}(exp)	E_{h0}(cal)	E'_{h0}(cal)
240.6	412.3	396.0	378.9	0.55	0.54	0.554	0.552
297.9	484.9	473.5	461.2	0.55	0.54	0.560	0.559
350.3	552.6	543.2	534.1	0.53	0.54	0.565	0.564
398.4	613.8	606.8	598.9	0.53	0.53	0.569	0.568

[a] Temperatures are in °C and the superscript ′ indicates the cooling mode.

temperature dependence of the spectra may cause a different temperature dependence of the effective emissivity. The hysteresis of the calculated emissivity for both modes is negligible because the temperature difference is much smaller in comparison with that of the graphite-plate temperature. The results of the calculation are also listed in Table I.

As shown in the present investigation, the validity of heat capacity measurements by thermal radiation calorimetry (TRAC) has been confirmed both experimentally and theoretically. Below 200°C, however, a larger change in the emissivity will cause larger errors in the results. For blackening the specimen surface, therefore, it is desired to use other substances showing larger absorption in the far-infrared region. Boron nitride and silicon carbide are candidates for lower temperature range. On the other hand, it is confirmed that the present colloidal graphite, with a velvet-like surface, is an adequate substance for measurements above about 200°C.

6. CONCLUSION

The theoretical and experimental radiant power exchange coefficients (the "effective" emissivities) have been discussed by considering the geometrical configuration between the blackened surfaces facing each other. The experimental value of 0.54 ± 0.01 was obtained in the temperature range from 220 to 430°C for the present model configuration. A heat capacity measurement of copper by the TRAC in which both heating and cooling modes were considered was used to derive the value. The theoretical value of 0.56 ± 0.01 was estimated by considering the geometrical configuration factors and the total emissivity of the blackened surface, which was obtained from the spectral reflectivity. No significant hysteresis of the effective emissivity was observed for heating and cooling modes.

ACKNOWLEDGMENTS

The authors are grateful to Professor R. A. Cowley, Oxford University, for his useful discussion and also to R. P. Tye for his continuous encouragement on the present subject.

REFERENCES

1. K. Hisano and T. Yamamoto, in *Proc. 12th Japan Symp. Thermophys. Prop., Vol. 12* (Japan Society of Thermophysical Properties, Kyoto, 1991), p. 287.
2. K. Hisano and T. Yamamoto, *High Temp. High Press.* **25**:337 (1993).
3. K. Hisano, *Int. J. Thermophys.* **18**:535 (1997).
4. K. Hisano and F. Placido, *High Temp. High Perss.* **30** (1998), in press.
5. A. Cezairliyan, *J. Res. Natl. Bur. Stand.* **75C**:7 (1971).
6. H. C. Hottel and A. F. Sarofim, *Radiative Transfer* (McGraw–Hill, New York, 1967).
7. R. Siegel and J. R. Howell, *Thermal Radiation Heat Transfer* (McGraw–Hill, New York, 1972).
8. D. E. Gray (ed.), *American Institute Physics Handbook* (McGraw–Hill, New York, 1972).